Filamin-A and Rheological Properties of Cultured Melanoma Cells

Mark F. Coughlin, Marina Puig-de-Morales, Predrag Bursac, Matthew Mellema, Emil Millet, and Jeffrey J. Fredberg
Physiology Program, Department of Environmental Health, Harvard School of Public Health, Boston, Massachusetts

ABSTRACT Here we report the rheological properties of cultured hsFLNa (filamin-A)-expressing (FIL+) and hsFLNa-deficient (FIL−) melanoma cells. Using magnetic twisting cytometry over a wide range of probing frequencies, and targeting either cortical or deeper cytoskeletal structures, we found that differences in stiffness of FIL+ versus FIL− cells were remarkably small. When probed through deep cytoskeletal structures, FIL+ cells were, at most, 30% stiffer than FIL− cells, whereas when probed through more peripheral cytoskeletal structures FIL− cells were not different except at very high frequencies. The loss tangent, expressed as an effective cytoskeletal temperature, was systematically greater in FIL− than FIL+ cells, but these differences were small and showed that the FIL+ cells were only slightly closer to a solidlike state. To quantify cytoskeletal remodeling, we measured spontaneous motions of beads bound to cortical cytoskeletal structures and found no difference in FIL+ versus FIL− cells. Although mechanical differences between FIL+ and FIL− cells were evident both in cortical and deeper structures, these differences were far smaller than expected based on measurements of the rheology of purified actin-filamin solutions. These findings do not rule out an important contribution of filamin to the mechanical properties of the cortical cytoskeleton, but suggest that effects of filamin in the cortex are not exerted on the length scale of the probe used here. These findings would appear to rule out any important contribution of filamin to the bulk mechanical properties of the cytoplasm, however. Although filamin is present in the cytoplasm, it may be inactive, its mechanical effects may be small compared with other crosslinkers, or mechanical properties of the matrix may be dominated by an overriding role of cytoskeletal prestress.

INTRODUCTION

Human filamin-A (hsFLNa) is a widely expressed filamin isoform (1,2). The absence of hsFLNa in a human melanoma cell line leads to extension and retraction of hemispherical blebs from the cell surface (3,4). Pellets of consolidated hsFLNa-deficient melanoma cells have half the stiffness as pellets of hsFLNa-expressing melanoma cells (3). This loss of stiffness and surface stability is thought to effect higher cell functions; growth, motility, chemotaxis, and focal adhesion reinforcement are impaired in filamin-deficient compared to filamin-expressing melanoma cells (3,5).

In purified systems containing only actin filaments and filamin molecules, actin filaments intersect at nearly orthogonal angles (6,7). Orthogonal crosslinking of actin filaments by filamin provides an efficient mechanism to regulate bulk rheological properties. Actin filament networks with few or no filamin molecules exhibit fluidlike properties; they flow under the application of a constant shear stress (8–10) and exhibit a near-power-law dependence of dynamic stiffness on oscillatory frequency (8,10,11). The addition of relatively few filamin molecules changes the consistency of the network from a viscoelastic fluid to an elastic solid; the solution gelates (9,12), the dynamic stiffness remains nearly constant over 3–4 decades of oscillatory frequency (11,13), and a nearly elastic creep response is observed under constant shear stress (13). Associated with the decrease in frequency dependence with addition of filamin molecules is a disproportionate increase in network stiffness. Doubling the number of filamin molecules at a fixed actin concentration more than doubles the dynamic stiffness, with increases at low frequencies exceeding an order of magnitude (11).

In purified actin-filamin gel systems, no other crosslinkers are present, filamin is uniformly distributed, and the network is usually studied in a range of mechanical perturbations around the unstressed state. In the living cell, by contrast, other crosslinkers are present, filamin is nonuniformly distributed, and the cytoskeletal network is under substantial tension (14). Imaging studies indicate that filamin-A concentrates mainly in the dense cortical cytoskeleton, although it has a wide spatial distribution throughout the cytoplasm (15–17). Moreover, imaging studies are unable to determine what fraction of the filamin in any cell region is bound to actin, active, and exerting mechanical effects. In the mechanical properties of the living cell, therefore, the role of filamin and the locus of its action remain unclear. Here we report cytoskeletal rheology and remodeling in adherent hsFLNa-expressing (FIL+) and hsFLNa-deficient (FIL−) melanoma cells in culture. To probe these cells, we used magnetic microbeads (4.5-μm-diameter) that were coated so as to emphasize mechanical coupling either to cortical or to deeper cytoskeletal structures.

Submitted February 19, 2005, and accepted for publication November 15, 2005.

Mark F. Coughlin and Marina Puig-de-Morales contributed equally to this work.

Address reprint requests to Dr. Mark F. Coughlin, Tel.: 617-432-2610; E-mail: mcoughli@hsph.harvard.edu.

0006-3495/06/03/2199/07 $2.00

doi: 10.1529/biophysj.105.061267

METHODS

Cell culture

Cells from a human melanoma cell line that do not express hsFLNa and cells from a subline that express hsFLNa after stable transfection of hsFLNa cDNA (3) were kindly provided by Y. Ohta (Hematology Division, Brigham and Women's Hospital; Harvard Medical School). Cells were plated in plastic culture flasks and maintained in minimum essential medium (Sigma, St. Louis, MO), supplemented with 8% newborn calf serum (Gibco, Gaithersburg, MD), 2% fetal calf serum (Sigma), 100 U/ml penicillin-streptomycin (Sigma), 10 mM HEPES (Gibco), and 0.03% sodium bicarbonate (Gibco). Media for FIL+ cells also contained 0.5 mg/ml of G418 (Gibco).

Filamin-A expression

Lysates were prepared for immunoblotting by harvesting cells at 80% confluency from six-well plates. Cells were trypsinized, suspended in serum-containing media, centrifuged, and washed with PBS to remove serum proteins, and suspended in homogenization buffer (20 mM Tris buffer, pH 7.6, 1 mM EGTA, 0.5 mM $MgSO_4$, 10 μg/ml leupeptin, 5 μg/ml pepstatin A, 10 μg/ml aprotinin, and 0.2 mM AEBSF [4-{2-aminoethyl}benzenesulfonyl fluoride]). Cells were homogenized by 20 passes with a small-volume Teflon-on-glass Dounce homogenizer and by two freeze-thaw cycles.

Protein concentration of the supernatant was determined by the Bradford method using Bio-Rad dye reagent (Bio-Rad, Richmond, CA). Supernatant of cell lysates were then mixed with loading buffer (0.062 M Tris-HCl, pH 6.8, 10% glycerol, 2% SDS, 5% b-mercaptoethanol, and 0.01% (wt/vol) bromphenol blue) to a volume of 30 ml and boiled for 5 min. Equal amounts of total cell protein (20 μg) were resolved by SDS-PAGE (125 V, 90 min) on 12% Tris-glycine gel (Invitrogen, Carlsbad, CA) and transferred to nitrocellulose membrane (20 V, 90 min) in transfer buffer (Invitrogen). Membranes were treated with blocking solution (10 mM Tris saline buffer containing 150 mM NaCl, 0.1% Tween 20, and 5% nonfat dry milk), incubated overnight at 4°C with primary mouse antibody to Filamin-A (MAB 1680, dilution of 1:1000; Chemicon, Temecula, CA), incubated for 1 h at room temperature with secondary goat anti-mouse IgG linked to horseradish peroxidase (dilution 1:1000; Cell Signaling, Woburn, MA), and then visualized by light emission on film with enhanced chemiluminescent substrate (Cell Signaling, Beverly, MA). The band visualized at ~25 kDa was scanned with a UMAX PowerLook flatbed scanner (Bio-Rad, Hercules, CA) and analyzed by scanning densitometry with Gel Pro Analyzer software (Media Cybernetics, Silver Spring, MD).

Filamin immunofluorescence

Cells were prepared for experiments as described below. Instead of assessing mechanical properties, the cells were fixed with 3.7% paraformaldehyde (Sigma) for 15 min, and permeabilized with 0.01% Triton-X (Sigma) for 15 min. Nonspecific staining was blocked with 10% normal goat serum (Sigma) and 1% BSA (Sigma) for 30 min. Filamin was stained by fluorescently tagged filamin antibody (Chemicon, Temecula, CA) at a dilution of 1:100 for 1 h at room temperature and mounted for immunofluorescence microscopy.

Ferrimagnetic microbeads

Ferrimagnetic beads (solid Fe_3O_4, 4.5-μm-diameter) were produced in our laboratory and their surfaces were treated in one of two ways. One set of beads was coated with a synthetic peptide containing the sequence RGD (Peptite 2000; Integra LifeSciences, San Diego, CA) at 50 μg ligand/mg beads by incubating beads overnight at 4°C in carbonate buffer (pH 9.4). Ligation of receptors on the cell surface by RGD-coated beads induces a cascade of events including the assembly of a focal adhesion complex (18) and the recruitment of cytoskeletal proteins to the bead attachment site (19). The resulting focal adhesion complex provides the means to transmit mechanical deformation to the cytoskeleton and throughout the cell (20). Thus, RGD-coated beads probe deep cytoskeletal structures.

Another set of beads was coated with poly-L-lysine (PLL) by incubating overnight at 4°C in 0.01% (w/v) PLL solution (Sigma). The binding of PLL-coated beads to the cell surface is nonspecific and integrin-independent. Poly-L-lysine-coated adhesion substrates do not induce the formation of a focal adhesion complex (21) and PLL-coated beads do not recruit cytoskeletal proteins to the site of attachment. Thus, PLL-coated beads probe primarily cortical cytoskeletal structures.

Experimental protocols

Cells were trypsinized (0.25% trypsin and 1 mM EDTA; Sigma) and plated at 10^4 cells/well on uncoated glass bottom wells (MatTek, Ashland, MA). FIL+ and FIL− cells were plated for 2.5 and 3.5 h, respectively, to insure the cells contained equal amounts of polymerized actin (4). After plating, cells were washed twice with media, and either RGD- or PLL-coated beads were added to the media for 20 min at 37°C to allow binding to receptors on the cell surface. The wells were washed twice with media to remove unbound beads. The final concentration of beads was approximately one per cell. Finally, rheological measurements were performed or spontaneous nanoscale motions (SNM) were monitored as described below.

Magnetic twisting cytometry with optical detection (OMTC)

The experimental setup for OMTC measurements was described in detail elsewhere (22,23). Briefly, glass-bottom wells containing cells with attached beads were placed on the stage of an inverted microscope (Leica Model #DM IRBE, Leica Microsystems, Wetzlar, Germany) and viewed under bright-field with 20× objective (NA = 0.4). Beads were first magnetized horizontally and then subjected to a vertical oscillatory magnetic field. This oscillatory field induces a mechanical torque $T(t)$ that twists the bead toward the imposed field. The beads undergo a measurable lateral displacement in addition to a small rotation. The bead motions were tracked through images captured by CCD camera (Model #JAI CV-M10, JAI PULNiX, San Jose, CA) with exposure time of 0.1 ms and acquisition frequency of 12 Hz. From recorded images, the bead position $r(t)$ was computed using an intensity-weighted center-of-mass algorithm yielding accuracy in $r(t)$ >5 nm (22). Measurements were performed at oscillatory frequencies between 10^{-1} and 10^3 Hz with heterodyning employed at twisting frequencies above 0.7 Hz.

Complex elastic moduli g^* of the cells were computed from the magnetic torque $T(t)$ and corresponding lateral bead motion $r(t)$ as described (22), using

$$g* = \bar{T}/\bar{r}- = g' + i\,g'', \tag{1}$$

where $i^2 = -1$ and an overbar indicate Fourier transformation. The modulus as defined has units of Pa/nm. A traditional modulus G^* is obtained from g^* by a multiplicative geometric scaling factor $\alpha = 6.8$ μm determined using a finite element model (24,25). This scaling depends on several factors, including bead size and the interaction between the bead and cell; however, the data from both FIL+ and FIL– cells are scaled by the same factor.

Beads were selected for analysis based on several criteria. Only individual beads attached to the apical surface of a cell were analyzed. As described previously (22), beads were included for further analysis, provided the amplitude of their motion (~20 nm) appreciably exceeded the system noise level, the motion resembled a sinusoidal waveform, and higher harmonics (nonlinearities) were not present. Beads were also discarded if they produced an unrealistic modulus measurement (e.g., a nonpositive g') even at only a single frequency. Typically 60–75% of the beads meet these criteria, although the exact number depended on the cell type and bead coating.

Spontaneous nanoscale motions (SNM)

To complement the rheological measurements on FIL+ and FIL− cells, the spontaneous motion of beads tightly bound to the cytoskeleton were tracked under the conditions of no external forcing. Beads cannot move unless the underlying cytoskeletal structures to which the bead is connected rearrange and remodel. Thus, SNMs report cytoskeletal remodeling (26,27).

The SNMs of RGD- or PLL-coated beads were observed under bright-field with a 40× objective (NA = 0.55). Bead positions were computed from images captured at 12 frames/s as described for OMTC measurements. Each bead was tracked for 341 s through 4096 images. The SNM were quantified by calculating the mean-square bead displacement (MSD) as

$$MSD(\Delta t) = \langle r^2(\Delta t)\rangle = \langle [r(t+\Delta t) - r(t)]^2\rangle, \qquad (2)$$

where Δt is the time lag between observations, and $\langle . \rangle$ denotes an average over many starting times t over the time course of observation.

To account for the contribution of stage drift and system noise to the MSD measurements, the SNMs of beads immobilized in epoxy were measured. The contribution to MSD of the cell was computed by subtracting the average MSD of beads in epoxy from the average MSD of beads on cells.

Effective cytoskeletal temperature

We have proposed recently that cytoskeletal dynamics may fit within the framework of molecular trapping in deep energy wells and molecular hopping out of those wells driven by an effective matrix temperature (23,25,26,28). This framework is simple, attractive, and fits all published observations. The effective cytoskeletal temperature x is experimentally accessible and has been shown recently to be a major factor controlling the rate of molecular-scale cytoskeletal rearrangements (26). The effective cytoskeletal temperature of FIL+ and FIL− cells was computed from the slope of the linear regression through the log G' versus log f data.

Statistics

The computed dynamic moduli at each frequency were log-normally distributed. To test for statistical differences in G' and G'' distributions between FIL+ and FIL− cells, we computed the logarithm of the data and compared the mean values by Student's t-test. The mean values of MSD at each time lag and effective cytoskeletal temperature between cell types were compared by Student's t-test. In all cases, probability values <0.05 were considered significantly different.

RESULTS

We confirmed that FIL+ cells express hsFLNa whereas FIL− cells do not, by Western immunoblotting, using an antibody raised against filamin-A (Fig. 1). FIL+ cells showed strong immunoreactivity for this filamin isoform and demonstrated little blebbing, whereas FIL− cells had no detectable filamin-A signal and demonstrated extensive blebbing. Staining for filamin-A in FIL+ cells revealed fluorescence throughout the cell and a strong signal around surface-bound beads (Fig. 2).

When we probed the cells using beads coated with RGD, the storage modulus (G') of FIL+ and FIL− cells increased as a power law of the oscillatory frequency (f) (Fig. 3 *A*). The loss modulus (G'') varied little with f below ~10 Hz (Fig. 3 *B*) before increasing rapidly at higher frequencies as the viscous contribution to G'' became dominant. The frequency dependence of G' and G'' observed in FIL+ and FIL− cells

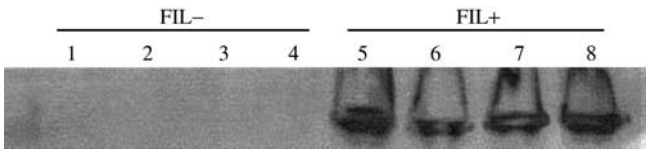

FIGURE 1 Western immunoblotting of total cell lysates from hsFLNa-expressing (FIL+) and hsFLNa-deficient (FIL–) melanoma cells. Cell lysates were probed via SDS-PAGE and Western immunoblotting using an antibody raised against Filamin-A. FIL– cells (Lanes *1–4*) have no detectable filamin-A signal, whereas the FIL+ cells (lanes *5–8*) show strong immunoreactivity for this filamin isoform. Equal amounts (20 μg) of total protein were loaded in each lane.

probed by RGD-coated beads is qualitatively similar to those measured in a variety of other cell types (25,29). Moreover, purified protein systems of actin filaments crosslinked by filamin molecules exhibit a near-power-law dependence of G' on f (8,10,11) and an increasing frequency dependence of G'' at high f (8).

Despite the presence of hsFLNa in FIL+ but not FIL− cells, G' and G'' of FIL+ and FIL− cells differed little in value or frequency dependence. The median G' of FIL+ cells exceeded FIL− cells by ~25%, except at $f = 100$ and 300 Hz, where the values were not different (Fig. 3 *A*). The median G'' of FIL+ cells exceeded FIL− cells at $f = 0.1$ Hz, whereas the opposite was true for f above 100 Hz where G'' of FIL− cells exceeded FIL+ cells. Little qualitative change was seen in the frequency dependence of G' and G'' in FIL+ compared to FIL− cells.

When we probed the cell using beads coated with PLL, as opposed to RGD, the moduli measured were substantially smaller, typically by threefold, but otherwise results were much the same. The storage modulus G' increased as a power law of f (Fig. 4 *A*), and G'' varied little with f below ~10 Hz, before increasing more rapidly at higher f (Fig. 4 *B*). No difference between G' of FIL+ and FIL− cells was

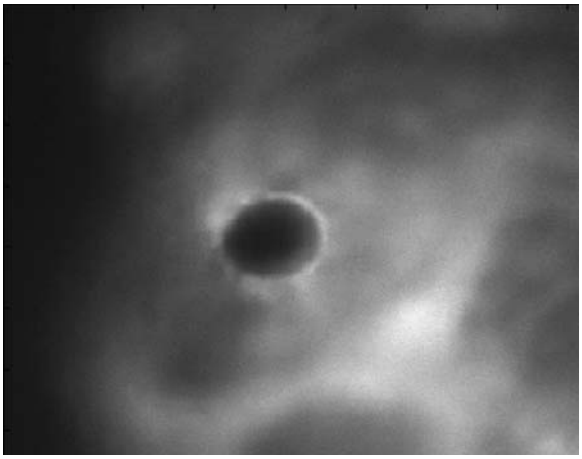

FIGURE 2 Immunofluorescent signal from a hsFLNa-expressing melanoma cell stained with antibodies to FLNa and binding a surface-bound RGD-coated bead. Note bright immunofluorescent signal from hsFLNa in the immediate vicinity of the bead above the diffuse background signal from hsFLNa located throughout the cytoplasm.

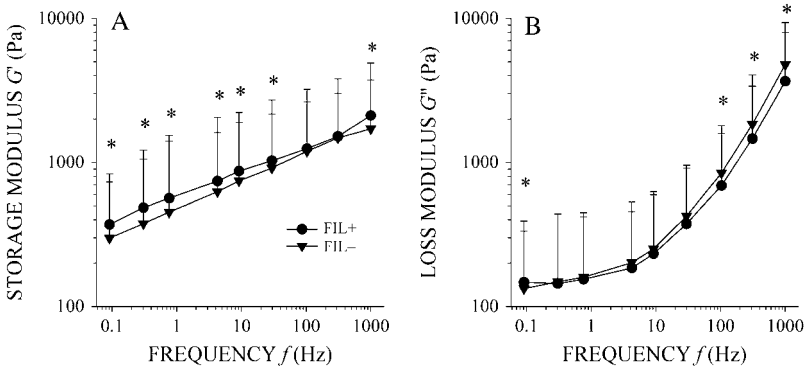

FIGURE 3 (*A*) Storage modulus (G') and (*B*) loss modulus (G'') as a function of frequency (f) for hsFLNa-expressing (FIL+) and hsFLNa-deficient (FIL−) melanoma cells probed by RGD-coated beads. Storage modulus of both FIL+ and FIL− cells exhibits power-law f-dependence with G' of FIL+ exceeding FIL– cells, except at $f = 100$ and 300 Hz. Loss modulus of both FIL+ and FIL− cells exhibits weak f-dependence at low f, where G'' of FIL+ exceed FIL– cells, and strong f-dependence at high f, where G'' of FIL– exceed FIL+ cells. Statistical significance ($P < 0.05$) is denoted by *. Data are median ± SD.

observed, except between $f = 30$ and 300 Hz where, surprisingly, G' of FIL– cells exceeded that of FIL+ cells. The loss modulus of FIL– cells systematically exceeded FIL+ cells for f at frequencies in excess of 0.7 Hz.

Mean-square displacement of RGD- and PLL-coated beads on FIL+ and FIL– cells exhibited subdiffusive behavior at small Δt (i.e., the local logarithmic slope of $\langle r(t)^2 \rangle$ vs. Δt was <1) and superdiffusive behavior at large Δt (i.e., the local logarithmic slope was >1) (Fig. 5). Subdiffusive behavior at small Δt and superdiffusive behavior at large Δt is consistent with the MSD of surface-bound beads from other cell lines (26,27). The mean MSD of RGD-coated beads on FIL+ cells was less than FIL− cells in the subdiffusive regime before becoming identical in the superdiffusive regime. No differences in the mean MSD of PLL-coated beads were observed between FIL+ and FIL– cells over all observed time lags.

DISCUSSION

When probed through RGD-coated beads, FIL+ compared to FIL− cells revealed 25% higher stiffness (Fig. 3 *A*). When probed through PLL-coated beads, except at high frequencies, they showed no detectable differences (Fig. 4 *A*). With either RGD- or PLL-coated beads, there was no prominent difference between FIL+ and FIL– cells in the frequency dependence of G' or G'', and only slight differences in spontaneous bead motions. Although mechanical differences between FIL+ and FIL– cells were evident both in cortical and deeper structures, these differences were far smaller than expected, based on measurements of the rheology of purified actin-filamin solutions.

These rheological measurements from FIL+ and FIL– cells stand in contrast to the behavior of unstressed purified actin filament networks where filamin crosslinking dramatically increases elastic moduli and changes the rheological properties from a viscoelastic fluid to an elastic solid. The molar ratios of actin to filamin in FIL+ and FIL– cells is ~160:1 and ~1000:1, respectively (3). In reconstituted actin-filamin gels at these molar ratios, the stiffness of the FIL+ gel is greater than the FIL– gel by 3.5-fold at higher frequencies (2 Hz) and 10-fold at lower frequencies (0.1 Hz) (11), and the frequency dependence from 0.01 to 2 Hz of the FIL+ gel is smaller (11).

What factors might account for the limited mechanical differences between FIL+ and FIL– cells? The first possibility to consider is methodological; the effect of filamin may not be exerted on the length scale of the probe used here. Although filamin is widely distributed in the cell (17,30), it is primarily located in the cortical cytoskeleton (15) where it provides mechanical support to the membrane (4). Our magnetic beads (4.5 μm-diameter) are large compared to the thickness of this filamin-containing cortical layer. Although we used either RGD- or PLL-coated beads to emphasize deeper versus cortical cytoskeletal structures, respectively, the size of our beads may limit our ability to probe only the

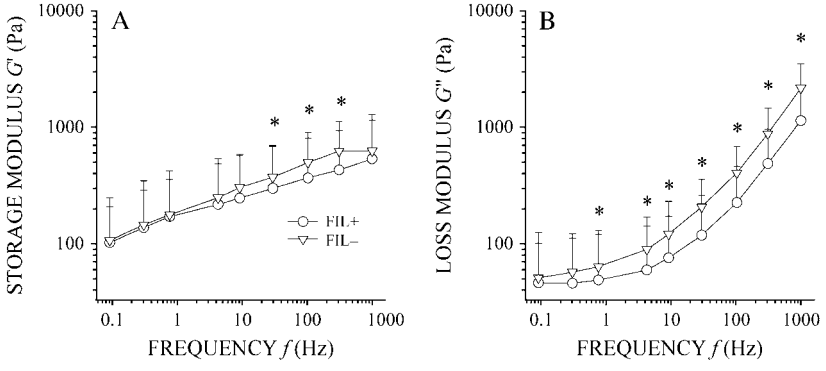

FIGURE 4 (*A*) Storage modulus (G') and (*B*) loss modulus (G'') as a function of frequency (f) for hsFLNa-expressing (FIL+) and hsFLNa-deficient (FIL−) melanoma cells probed by poly-L-lysine-coated beads. Storage modulus of both FIL+ and FIL− cells exhibits near-power-law f-dependence with G' of FIL– exceeding FIL+ cells between $f = 30$ and 300 Hz. Loss modulus of both FIL+ and FIL− exhibits strong f-dependence with G'' of FIL– exceeding FIL+ cells above $f = 0.7$ Hz. Statistical significance ($P < 0.05$) is denoted by *. Data are median ± SD.

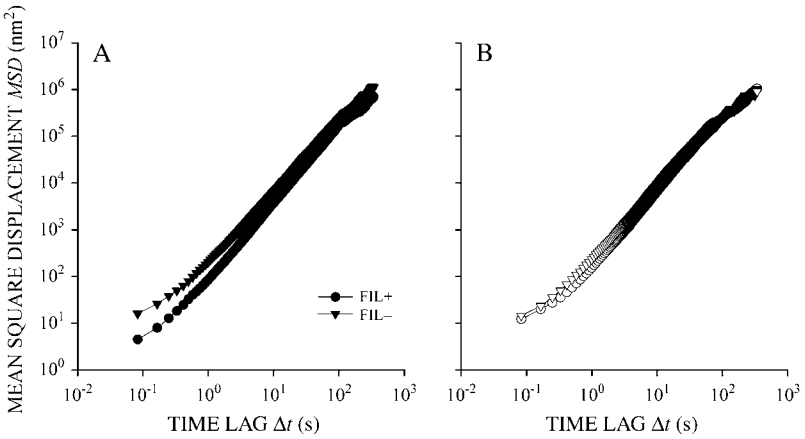

FIGURE 5 Mean-square displacement (MSD) as a function of the time lag (Δt) of hsFLNa-expressing (FIL+) and hsFLNa-deficient (FIL−) cells probed by (*A*) RGD- and (*B*) poly-L-lysine (PLL)-coated beads. Mean-square displacement of RGD- and PLL-coated beads on FIL+ and FIL− cells exhibited subdiffusive behavior at small Δt and superdiffusive behavior at large Δt. With RGD-coated beads, MSD of FIL− exceeded FIL+ cells below $\Delta t = 33$ s. With PLL-coated beads, MSD of FIL+ and FIL− cells were not different. Data are mean ± SD.

thin cortical region where filamin is thought to play its major mechanical role. Thus, our measurements may reveal little mechanical effect of filamin because they do not probe regions of the cell where filamin is most important. Nonetheless, the findings of small rheological differences in FIL+ versus FIL− cells at the scale probed here are consistent with the small differences detected using other mechanical assays; the force required to pull a membrane tether out of FIL+ cells is only ~10% higher than FIL− cells (31), and cytoskeletal reinforcement of collagen-coated beads is greater in FIL+ than FIL− cells, but other measures (MSD) show no differences (32).

The second possibility to consider is that crosslinking by other filamin isoforms or other actin-binding proteins might account for the small mechanical differences in FIL+ and FIL− cells. Overexpression of hsFLNb may compensate for missing hsFLNa in living cells (33). Even the actin-associated proteins whose level of expression was unchanged by hsFLNa transfection (3) may compensate for missing hsFLNa if their actin-binding activity in FIL− cells is altered. Yet, the FIL− cells continue blebbing, suggesting that hsFLNa is not completely compensated for by other cytoskeletal or actin-binding proteins.

The third possibility is that crosslinking of actin by filamin may not be a primary determinant of cell shape stability and rheology. Until these cells are profiled genetically or proteomically, it remains unknown what other important cytoskeletal proteins might differ between the cell lines. Another possibility is that cell shape stability and rheology is determined by cytoskeletal prestress (14,34). In our measurements, FIL+ and FIL− cells are adherent and their cytoskeletal prestress is born by the underlying substrate. When detached FIL+ and FIL− cells are probed in the absence of prestress, their stiffness is low, and the stiffness of FIL+ cells is more than double that of the FIL– cells (3).

Further support for the importance of the prestress comes from recent in vitro measurements on actin-filamin gels (M. L. Gardel, F. Nakumara, J. H. Hartwig, J. C. Crocker, T. P. Stossel, and D. A. Weitz, unpublished data) showing that actin-filamin gels mimic the major rheological features of FIL+ and FIL− cells reported here, but only if the gel is subjected to an appreciable prestress. Moreover, the stiffness of the prestressed actin-filamin gel is insensitive to filamin concentration. Taken together, these observations in living cells and inert gels are mutually consistent and mutually reinforcing.

Another interesting feature of the rheology of FIL+ and FIL− cells is that they exhibit characteristics of soft glassy materials (25,26,35,36). A key concept from the theory of soft glassy rheology is that of an effective temperature, x. The effective temperature is indicative of the level of mechanical agitation in the stress-bearing elements of the cytoskeletal lattice and seems to play a major role in the rate of structural rearrangements (26,35). Moreover, as x varies between $1 \leq x \leq 2$, the rheological properties of the material vary between that of a Hookean elastic solid and a Newtonian viscous fluid. Despite the remarkably similar rheological properties of FIL+ and FIL− cells (Figs. 3 and 4), the mean value of x was higher in FIL− than FIL+ cells

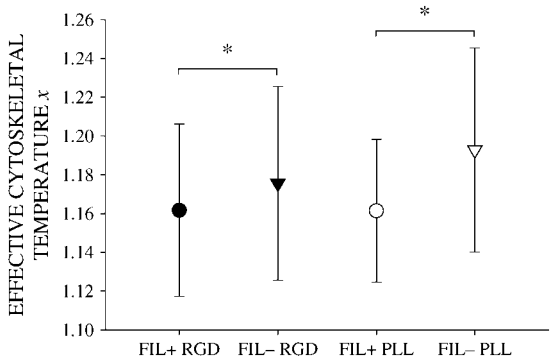

FIGURE 6 Effective cytoskeletal temperature (x) of hsFLNa-expressing (FIL+) and hsFLNa-deficient (FIL−) melanoma cells probed by RGD- (*solid symbols*) or poly-L-lysine-coated (PLL) beads (*open symbols*). Effective cytoskeletal temperature was higher in FIL− than FIL+ cells when probed by either RGD- or PLL-coated beads. Statistical significance ($P < 0.05$) is denoted by *. Data are mean ± SD.

when probed by either RGD- or PLL-coated beads (Fig. 6). This suggests that hsFLNa makes FIL+ cells more solidlike ($x \rightarrow 1$), but the difference was small. The finding that x is higher in the more mechanically agitated (blebbing) FIL− cells than the more stable FIL+ cells is consistent with the notion that x reflects the level of mechanical agitation in stress-bearing elements.

Although no prominent mechanical role for hsFLNa was found in rheological measurements, MSD measurements revealed that filamin may have a role in controlling the rate of structural rearrangements. Differences in MSD between FIL+ cells and FIL– cells were detected with RGD- but not PLL-coated beads (Fig. 5). This suggests that the rate of structural rearrangements in FIL+ and FIL– cells differed within deep cytoskeletal structures, with the rate in FIL– cells exceeding FIL+ cells.

CONCLUSIONS

Mechanical differences between FIL+ and FIL− cells were evident both in cortical and deeper structures, but these differences were far smaller than expected based on measurements of the linear rheology of purified actin-filamin solutions. These findings do not rule out an important contribution of filamin to the mechanical properties of cortical cytoskeleton, but suggest that effects of filamin in the cortex are not exerted on the length scale of the probe used here. These findings would appear to rule out any important contribution of filamin to the bulk mechanical properties of the cytoplasm, however. Although filamin is present in the cytoplasm, it may be inactive, its mechanical effects there may be small compared with other crosslinkers, or mechanical properties of the matrix may be dominated by an overriding role of the cytoskeletal prestress.

We thank Dr. Y. Ohta (Hematology Division, Brigham and Women's Hospital; Harvard Medical School) for providing the melanoma cells, and Drs. T. Stossel (Hematology Division, Brigham and Women's Hospital; Harvard Medical School), B. Fabry (University of Erlangen), G. Lenormand (Harvard School of Public Health), and R. Laudadio (Harvard School of Public Health) for helpful discussions.

This work was supported by grant Nos. HL33009, HL59682, and HL65960.

REFERENCES

1. Stossel, T. P., J. Condeelis, L. Cooley, J. H. Hartwig, A. Noegel, M. Schleicher, and S. S. Shapiro. 2001. Filamins as integrators of cell mechanics and signalling. *Nat. Rev. Mol. Cell Biol.* 2:138–145.
2. van der Flier, A., and A. Sonnenberg. 2001. Structural and functional aspects of filamins. *Biochim. Biophys. Acta.* 1538:99–117.
3. Cunningham, C. C., J. B. Gorlin, D. J. Kwiatkowski, J. H. Hartwig, P. A. Janmey, R. Byers, and T. P. Stossel. 1992. Actin-binding protein requirement for cortical stability and efficient locomotion. *Science.* 255:325–327.
4. Cunningham, C. C. 1995. Actin polymerization and intracellular solvent flow in cell surface blebbing. *J. Cell Biol.* 129:1589–1599.
5. Glogauer, M., P. Arora, D. Chou, P. A. Janmey, G. P. Downey, and C. A. G. McCulloch. 1998. The role of actin-binding protein 280 in integrin-dependent mechanoprotection. *J. Biol. Chem.* 273:1689–1698.
6. Hartwig, J. H., J. Tyler, and T. P. Stossel. 1980. Actin-binding protein promotes the bipolar and perpendicular branching of actin filaments. *J. Cell Biol.* 87:841–848.
7. Neiderman, R., P. C. Amrein, and J. Hartwig. 1983. Three-dimensional structure of actin filaments and of an actin gel made with actin-binding protein. *J. Cell Biol.* 96:1400–1413.
8. Goldmann, W. H., M. Temple, I. Sprenger, G. Isenberg, and R. M. Ezzell. 1997. Viscoelasticity of actin-gelsolin networks in the presence of filamin. *Eur. J. Biochem.* 246:373–379.
9. Nunnally, M. H., L. D. Powell, and S. W. Craig. 1981. Reconstitution and regulation of actin gel-sol transformation with purified filamin and villin. *J. Biol. Chem.* 256:2083–2086.
10. Zaner, K. S. 1986. The effect of the 540-kiloDalton actin cross-linking protein, actin-binding protein, on the mechanical properties of F-actin. *J. Biol. Chem.* 261:7615–7620.
11. Tseng, Y., K. M. An, O. Esue, and D. Wirtz. 2004. The bimodal role of filamin in controlling the architecture and mechanics of F-actin networks. *J. Biol. Chem.* 279:1819–1826.
12. Brotschi, E. A., J. H. Hartwig, and T. P. Stossel. 1978. The gelation of actin by actin-binding protein. *J. Biol. Chem.* 253:8988–8993.
13. Janmey, P. A., S. Hvidt, J. Lamb, and T. P. Stossel. 1990. Resemblance of actin-binding protein/actin gels to covalently crosslinked networks. *Nature.* 345:89–92.
14. Wang, N., I. M. Tolić-Nørrelykke, J. Chen, S. M. Mijailovich, J. P. Butler, J. J. Fredberg, and D. Stamenović. 2002. Cell prestress. I. Stiffness and prestress are closely associated in adherent contractile cells. *Am. J. Cell. Physiol.* 282:C606–C616.
15. Hartwig, J. H., and P. Shevlin. 1986. The architecture of actin filaments and the ultrastructural location of actin-binding protein in the periphery of lung macrophages. *J. Cell Biol.* 103:1007–1020.
16. Flanagan, L. A., J. Chou, H. Falet, R. Neujahr, J. H. Hartwig, and T. P. Stossel. 2001. Filamin A, the Arp2/3 complex, and the morphology and function of cortical actin filaments in human melanoma cells. *J. Cell Biol.* 155:511–517.
17. Ohta, Y., N. Suzuki, S. Nakamura, J. H. Hartwig, and T. P. Stossel. 1999. The small GTPase RalA targets filamin to induce filopodia. *Proc. Natl. Acad. Sci. USA.* 96:2122–2128.
18. Wang, N., J. P. Butler, and D. E. Ingber. 1993. Mechanotransduction across the cell surface and through the cytoskeleton. *Science.* 260: 1124–1127.
19. Deng, L. H., N. J. Fairbank, B. Fabry, P. G. Smith, and G. N. Maksym. 2004. Localized mechanical stress induces time-dependent actin cytoskeletal remodeling and stiffening in cultured airway smooth muscle cells. *Am. J. Physiol. Cell Physiol.* 287:C440–C448.
20. Hu, S., J. Chen, B. Fabry, Y. Numaguchi, A. Gouldstone, D. E. Ingber, J. J. Fredberg, J. P. Butler, and N. Wang. 2003. Intracellular stress tomography reveals stress focusing and structural anisotropy in cytoskeleton of living cells. *Am. J. Physiol. Cell Physiol.* 285:C1082–C1090.
21. Riveline, D., E. Zamir, N. Q. Balaban, U. S. Schwarz, T. Ishizaki, S. Narumiya, Z. Kam, B. Geiger, and A. D. Bershadshy. 2001. Focal contacts as mechanosensors: externally applied local mechanical force induces growth of focal contacts by an mDia1-dependent and ROCK-independent mechanism. *J. Cell Biol.* 153:1175–1185.
22. Fabry, B., G. N. Maksym, S. A. Shore, P. E. Moore, J. Reynold, A. Panettieri, J. P. Butler, and J. J. Fredberg. 2001. Time course and heterogeneity of contractile responses in cultured human airway smooth muscle cells. *J. Appl. Physiol.* 91:986–994.
23. Fabry, B., G. N. Maksym, J. P. Butler, M. Glogauer, D. Navajas, N. A. Taback, E. J. Millet, and J. J. Fredberg. 2003. Timescale and other invariants of integrative mechanical behavior in living cells. *Phys. Rev. E.* 68:041914.

24. Mijailovich, S. M., M. Kojic, M. Zivkovic, B. Fabry, and J. J. Fredberg. 2002. A finite element model of cell deformation during magnetic bead twisting. *J. Appl. Physiol.* 93:1429–1436.

25. Fabry, B., G. N. Maksym, J. P. Butler, M. Glogauer, D. Navajas, and J. J. Fredberg. 2001. Scaling the microrheology of living cells. *Phys. Rev. Lett.* 87:148102.

26. Bursac, P., G. Lenormand, B. Fabry, M. Oliver, D. A. Weitz, V. Viasnoff, J. P. Butler, and J. J. Fredberg. 2005. Cytoskeletal remodelling and slow dynamics in the living cell. *Nat. Mater.* 4:557–561.

27. An, S. S., B. Fabry, M. Mellema, P. Bursac, W. T. Gerthoffer, U. S. Kayyali, M. Gaestel, S. A. Shore, and J. J. Fredberg. 2004. Role of heat shock protein 27 in cytoskeletal remodeling of the airway smooth muscle cell. *J. Appl. Physiol.* 96:1701–1713.

28. Fabry, B., and J. J. Fredberg. 2003. Remodeling of the airway smooth muscle cell: are we built of glass? *Respir. Physiol. Neurobiol.* 137: 109–124.

29. Puig-de-Morales, M., E. Millet, B. Fabry, D. Navajas, N. Wang, J. P. Butler, and J. J. Fredberg. 2004. Cytoskeletal mechanics in the adherent human airway smooth muscle cells: probe specificity and scaling of protein-protein dynamics. *Am. J. Physiol. Cell Physiol.* 287:C643–C654.

30. Langanger, G., J. D. Mey, M. Moeremans, G. Daneels, M. D. Brabander, and J. V. Small. 1984. Ultrastructural localization of α-actinin and filamin in cultured cells with the immunogold staining (IGS) method. *J. Cell Biol.* 99:1324–1334.

31. Dai, J., and M. P. Sheetz. 1999. Membrane tether formation from blebbing cells. *Biophys. J.* 77:3363–3370.

32. Giannone, G., G. Jiang, D. H. Sutton, D. R. Critchley, and M. P. Sheetz. 2003. Talin1 is critical for force-dependent reinforcement of initial integrin-cytoskeleton bonds but not tyrosine kinase activation. *J. Cell Biol.* 163:409–419.

33. Sheen, V. L., Y. Feng, D. Graham, T. Takafuta, S. S. Shapiro, and C. A. Walsh. 2002. Filamin A and filamin B are co-expressed within neurons during periods of neuronal migration and can physically interact. *Human Mol. Gen.* 11:2845–2854.

34. Stamenović, D., B. Suki, B. Fabry, N. Wang, and J. J. Fredberg. 2004. Rheology of airway smooth muscle cells is associated with cytoskeletal contractile stress. *J. Appl. Physiol.* 96:1600–1605.

35. Sollich, P. 1998. Rheological constitutive equation for a model of soft glassy materials. *Phys. Rev. E.* 58:738–759.

36. Fielding, S. M., P. Sollich, and M. E. Cates. 2000. Aging and rheology in soft materials. *J. Rheol.* 44:323–369.